Monthly Notices
of the
ROYAL ASTRONOMICAL SOCIETY

MNRAS **496,** L127–L132 (2020)
Advance Access publication 2020 June 1

doi:10.1093/mnrasl/slaa103

The universal acceleration scale from stellar feedback

Michael Y. Grudić [1,2]★ Michael Boylan-Kolchin [3]
Claude-André Faucher-Giguère [1] and Philip F. Hopkins [2]

[1]*Department of Physics and Astronomy and CIERA, Northwestern University, 2145 Sheridan Road, Evanston, IL 60208, USA*
[2]*TAPIR, California Institute of Technology, Mailcode 350-17, Pasadena, CA 91125, USA*
[3]*Department of Astronomy, The University of Texas at Austin, 2515 Speedway, Stop C1400, Austin, TX 78712, USA*

Accepted 2020 April 17. Received 2020 April 10; in original form 2019 October 23

ABSTRACT

It has been established for decades that rotation curves deviate from the Newtonian gravity expectation given baryons alone below a characteristic acceleration scale $g_\dagger \sim 10^{-8}\,\mathrm{cm\,s^{-2}}$, a scale promoted to a new fundamental constant in MOND. In recent years, theoretical and observational studies have shown that the star formation efficiency (SFE) of dense gas scales with surface density, SFE $\sim \Sigma/\Sigma_{\rm crit}$ with $\Sigma_{\rm crit} \sim \langle \dot{p}/m_* \rangle/(\pi G) \sim 1000\,\mathrm{M_\odot\,pc^{-2}}$ (where $\langle \dot{p}/m_* \rangle$ is the momentum flux output by stellar feedback per unit stellar mass in a young stellar population). We argue that the SFE, more generally, should scale with the local gravitational acceleration, i.e. that SFE $\sim g_{\rm tot}/g_{\rm crit} \equiv (G\,M_{\rm tot}/R^2)/\langle \dot{p}/m_* \rangle$, where $M_{\rm tot}$ is the total gravitating mass and $g_{\rm crit} = \langle \dot{p}/m_* \rangle = \pi G\,\Sigma_{\rm crit} \approx 10^{-8}\,\mathrm{cm\,s^{-2}} \approx g_\dagger$. Hence, the observed $g_\dagger$ may correspond to the characteristic acceleration scale above which stellar feedback cannot prevent efficient star formation, and baryons will eventually come to dominate. We further show how this may give rise to the observed acceleration scaling $g_{\rm obs} \sim (g_{\rm baryon}\,g_\dagger)^{1/2}$ (where $g_{\rm baryon}$ is the acceleration due to baryons alone) and flat rotation curves. The derived characteristic acceleration $g_\dagger$ can be expressed in terms of fundamental constants (gravitational constant, proton mass, and Thomson cross-section): $g_\dagger \sim 0.1\,G\,m_{\rm p}/\sigma_{\rm T}$.

Key words: galaxies: evolution – galaxies: formation – cosmology: dark matter.

1 INTRODUCTION

The kinematics of galaxies require something beyond the Newtonian gravity of baryonic matter (e.g. Rubin, Ford & Thonnard 1978, 1980; Bosma 1981a, b), an amazing observation that has moved from controversial to iron-clad over the past five decades (e.g. Bershady et al. 2011). In conjunction with observations of the cosmic microwave background and large-scale structure of the Universe (e.g. Planck Collaboration VI 2018), this observation has led to the commonly accepted idea that the mass content of the Universe is dominated by dark matter (DM). In the standard lambda cold dark matter (ΛCDM) cosmology, DM reconciles observations with the fact that, according to general relativity, Newtonian gravity should be valid throughout the Universe whenever gravitational fields are weak.

The effects of DM become important not at some characteristic radius, nor some characteristic galaxy mass, but at a critical *acceleration* scale. For gravitational accelerations $g \gg g_\dagger \approx 1.2 \times 10^{-8}\,\mathrm{cm\,s^{-2}}$, baryons dominate the gravitational dynamics of galaxies, while for $g \ll g_\dagger$, DM dominates. This led Milgrom (1983a, b, c) to propose that modifying Newton's law of gravity (or inertia) for very small accelerations, rather than DM, is the correct interpretation of galaxy dynamics. More recently, Lelli et al. (2017) have shown that the total gravitational acceleration in disc galaxies is well predicted by the acceleration provided by the baryons alone, with the acceleration scale $g_\dagger$ as the transition point from where the observed acceleration agrees with that of the baryons and below which some additional acceleration is required.

Some have suggested that a characteristic acceleration scale is an expected outcome of galaxy formation in ΛCDM. Kaplinghat & Turner (2002) argued that ΛCDM predicts galaxies to have an insensitive acceleration scale at the radius where the transition from baryon-dominated to DM-dominated occurs. However, Kaplinghat & Turner's derivation assumed (incorrectly) that most of the available baryons collapse into galactic discs in all DM haloes. This derivation therefore cannot account for low surface brightness galaxies that have acceleration $g < g_\dagger$ everywhere. van den Bosch & Dalcanton (2000) showed that semi-analytical galaxy models could be constructed within ΛCDM that exhibit the observed acceleration scale $g_\dagger$. They accounted for stellar feedback with a simple parametrized model, and found that these parameters could be tuned to put the model on observed galactic scaling relations. However, it was not clear whether stellar feedback actually acts

★ E-mail: mike.grudic@northwestern.edu

according to this model, and if so, how the value of $g_\dagger$ could be understood from basic principles or stellar evolution considerations.

Most recently, many cosmological galaxy formation simulations with baryonic physics have formed galaxies with rotation curves in good agreement with the radial acceleration relation (e.g. Santos-Santos et al. 2016; Keller & Wadsley 2017; Ludlow et al. 2017; Navarro et al. 2017; Garaldi et al. 2018; Dutton et al. 2019). As in van den Bosch & Dalcanton (2000)'s semi-analytical model, these simulation studies generally find feedback to be crucial for forming galaxies with realistic properties in ΛCDM. In the context of ΛCDM, it is clear that feedback is what connects the baryonic content of a disc galaxy to its DM halo and that this connection must be in some sense 'universal' to explain observed scaling relations. In this letter, we argue that stellar feedback in the form of momentum injection from massive stars can naturally explain the critical acceleration scale found in observations of disc galaxies, with that scale *built into* stellar physics and evolution, as opposed to arising from a coincidence or 'fine-tuning' of various effects.

2 PHYSICAL MODEL

2.1 Scaling of the star formation efficiency

Star formation efficiency (SFE), broadly speaking, is the mass in stars formed per mass in gas available for star formation. The SFE has numerous observational and theoretical definitions, depending on the spatial (e.g. galactic versus kpc scale versus cloud scale) and temporal (e.g. per free-fall time, per Gyr, or integrated) scales of interest, as well as the observational tracer used (e.g. young stellar objects, Hα). We refer to Krumholz, McKee & Bland-Hawthorn (2019) for a review of the SFE on giant molecular cloud/star cluster scales and to Kennicutt & Evans (2012) for galactic scales. For the simple discussion here, we define the SFE as the fraction of available gas mass converted to new stars during a given 'episode' of star formation, SFE $\equiv M_{*,\rm young}/M_{\rm gas,initial}$. The scaling of the SFE that results from a competition between gravity and stellar feedback has been extensively studied over the last few decades, both in the context of individual star-forming clouds and for entire galaxies (e.g. Larson 1974; Rees & Ostriker 1977; Dekel & Silk 1986; Silk 1997; Efstathiou 2000; Murray, Quataert & Thompson 2005, 2010; Fall, Krumholz & Matzner 2010). Below, we sketch a toy model that captures the core of our present understanding of self-regulated star formation.

Consider a 'patch' of gas in a galactic disc (or cloud) of mass $M_{\rm gas,initial}$ localized within a radius R, which is Jeans unstable and begins to cool and form stars. These stars will act back on the collapsing gas, injecting momentum at a rate per unit area $\dot{P}_{\rm fb}$, which is proportional to the mass of young stars (since the feedback is dominated by massive stars), $\dot{P}_{\rm fb} \sim \langle \dot{p}/m_* \rangle\, M_{*,\rm young}$ (where $\langle \dot{p}/m_* \rangle$ is the momentum injection rate per stellar mass formed). If this exceeds the weight of the gas $\sim G\, M_{\rm tot}\, M_{\rm gas}/R^2$ (where $M_{\rm tot}$ is the *total* mass localized within $<R$), then the gas becomes unbound, i.e. SF ceases and the remaining gas is ejected, when

$$\frac{M_{*,\rm young}}{M_{\rm gas,expelled}} \sim \frac{G\, M_{\rm tot}}{\langle \dot{p}/m_* \rangle\, R^2} = \frac{\Sigma_{\rm tot}}{\Sigma_{\rm crit}}, \tag{1}$$

where $\Sigma_{\rm tot} \equiv M_{\rm tot}/\pi R^2$ and $\Sigma_{\rm crit} \equiv \langle \dot{p}/m_* \rangle/(\pi\, G)$.

In recent years, a considerable body of work has explored the SFE and demonstrated that such a scaling, with a roughly constant $\Sigma_{\rm crit} \sim 1000\,{\rm M}_\odot\,{\rm pc}^{-2}$, works remarkably well at describing both observations (e.g. Wong et al. 2019) and detailed numerical simulations of cloud collapse (e.g. Hopkins, Quataert & Murray 2012a; Colín, Vázquez-Semadeni & Gómez 2013; Raskutti, Ostriker & Skinner 2016; Gavagnin et al. 2017; Grudić et al. 2018; Kim et al. 2018; Li et al. 2019). We compile in Fig. 1 SFE predictions for GMCs (or more generally 'ISM patches') from various simulations including stellar feedback, as well as recent observations of NGC 300 (Kruijssen et al. 2019). The compilation shows that there is an emerging consensus that the SFE scales linearly with $\Sigma_{\rm tot}$ over at least 2 dex in surface density, reaching $\sim$1 for $\Sigma_{\rm tot} \gtrsim \Sigma_{\rm crit}$.[1] Although model predictions vary at the factor of $\sim$2–3 level at fixed $\Sigma_{\rm tot}$, much of the scatter can be attributed to differences in initial conditions, definitions, and numerical methods (e.g. Geen et al. 2018; Grudić & Hopkins 2019; Hopkins & Grudić 2019).

Moreover, the ensemble and time-averaged version of this simple scaling can explain the observed Schmidt–Kennicutt relation in terms of $\langle \dot{p}/m_* \rangle$ (or its time-integrated equivalent $\langle p/m_* \rangle$; e.g. Silk 1997; Thompson, Quataert & Murray 2005; Hopkins, Quataert & Murray 2011; Ostriker & Shetty 2011; Faucher-Giguère, Quataert & Hopkins 2013; Semenov, Kravtsov & Gnedin 2016; Orr et al. 2018). Taken one step further, this also naturally leads to the scalings for momentum-conserving galactic outflows (e.g. Murray et al. 2005;

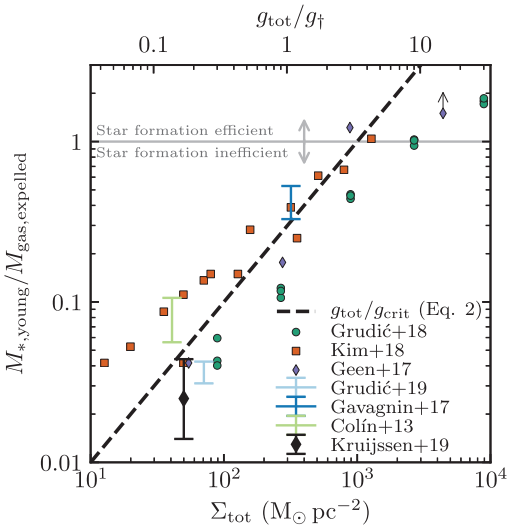

Figure 1. Ratio of the young stellar mass formed to the expelled gas mass in GMCs as a function of total mass surface density $\Sigma_{\rm tot}$, which is equivalent to an effective acceleration $g_{\rm tot} \equiv \pi G \Sigma_{\rm tot}$, plotted on top in units of $g_\dagger$ (the observed characteristic acceleration scale of galaxies). Kruijssen et al. (2019) is the one observational measurement presently available, and was made in NGC 300; all other points are theoretical results. The models generally predict that $M_{*,\rm young}/M_{\rm expelled} \to 1$ as $\Sigma_{\rm tot}$ exceeds $\Sigma_{\rm crit} \sim 10^3\,{\rm M}_\odot\,{\rm pc}^{-2}$, i.e. star formation becomes efficient. The theoretical results come from (magneto)hydrodynamic simulations (Colín, Vázquez-Semadeni & Gómez 2013; Gavagnin et al. 2017; Geen, Soler & Hennebelle 2017; Grudić et al. 2018, 2019; Kim, Kim & Ostriker 2018), and all include stellar feedback at least in the form of radiation from massive stars. The dashed line shows the simple analytical scaling from equation (2) for comparison. Error bars denote the full range of results obtained in studies that survey only one value of $\Sigma_{\rm eff}$ and vary either cloud mass or physics prescriptions.

[1] It is common in the star formation literature to define the SFE as $M_{*,\rm young}/(M_{\rm gas,expelled} + M_{*,\rm young})$, effectively neglecting the possibility of a significant DM component.

Hopkins, Quataert & Murray 2012b; Hayward & Hopkins 2017), with the same constant $\langle \dot{p}/m_* \rangle$ appearing.[2]

The value $\langle \dot{p}/m_* \rangle$ thus plays a critical and 'universal' role in star formation. It is important to note that the value of $\langle \dot{p}/m_* \rangle$ is similar regardless of whether radiation pressure, photoionization, or supernovae (SNe) dominate the feedback, as they all provide similar momentum injection rates for standard stellar population models (e.g. Leitherer et al. 1999; Bruzual & Charlot 2003; Hopkins et al. 2011; Agertz et al. 2013). Specifically, radiation pressure from a young stellar population contributes the specific momentum of photons, $\langle \dot{p}/m_* \rangle \approx c^{-1}\,(L/M)_{*,\,\rm young} \sim c^{-1}\,(1000\,L_\odot/M_\odot) \approx 6\times10^{-8}\,{\rm cm\,s^{-2}}$. The simulations of Colín et al. (2013), Kim et al. (2018), and Geen et al. (2017) predict a similar effective $\langle \dot{p}/m_* \rangle$ when including photoionization alone: this is generally understood to be because H II bubbles 'vent out' their energy in inhomogeneous GMCs, so this feedback channel also behaves effectively as a momentum-driven one. SNe from a given stellar population impart a momentum per unit stellar mass of $\sim$1000 km s^{-1}, nearly independent of ambient medium properties (e.g. Kim & Ostriker 2015; Martizzi, Faucher-Giguère & Quataert 2015), and within that population core-collapse SNe occur steadily until the last (i.e. least massive, $\sim$8 M$_\odot$) progenitors go off around 40 Myr. This again yields a momentum injection rate of $\langle \dot{p}/m_* \rangle \approx 1000\ {\rm km\,s^{-1}}/40\ {\rm Myr} \approx 6\times10^{-8}\ {\rm cm\,s^{-1}}$. Lastly, in standard stellar mass-loss models (which likely overestimate the effects of winds; Smith 2014), the momentum from stellar winds is at most comparable to that of photons.

Although myriad controversies and unsolved questions still remain in the study of star formation, this controversy has largely centred on the exact order-unity coefficients [e.g. the fraction of the momentum coupled versus 'vented,' corrections for turbulent media, cooling, and chemistry effects (Clark & Glover 2014), and non-linear time-dependent effects], and the question of which feedback mechanisms dominate on which spatial and time-scales. None of these effects are expected to alter the dimensional scaling in equation (1) at the level of our simplified explanation.

2.2 A characteristic acceleration scale from stellar feedback

For historical reasons, the convention in the star formation literature has been to express equation (1) in terms of a critical surface density and it is common to assume (e.g. in the context of individual molecular clouds) that $\Sigma_{\rm tot}$ is dominated by gas. This is the case for the numerical experiments cited in Section 2.1. However, let us now assume that those experiments substantiate the simple force-balance argument leading to equation (1), and that this can be generalized to a galactic context. This is not wholly certain, as these works neglect the galactic-scale context, which does imprint upon the morphologies and flow patterns of star-forming gas complexes in a manner that is more complex than in idealized set-ups (e.g. Rey-Raposo, Dobbs & Duarte-Cabral 2014). Our assumption is effectively that such additional effects should not alter the overall dimensional scaling in the problem, provided we recognize that the relevant acceleration should be the total gravitational acceleration including *all* matter, $g_{\rm tot} = G\,M_{\rm tot}/R^2$. With this definition, equation (1) can be rewritten as

$$\frac{M_{*,\,\rm young}}{M_{\rm gas,\,expelled}} \sim \frac{G\,M_{\rm tot}}{\langle \dot{p}/m_* \rangle\,R^2} = \frac{g_{\rm tot}}{g_{\rm crit}},$$
$$g_{\rm crit} \equiv \langle \dot{p}/m_* \rangle = \pi\,G\,\Sigma_{\rm crit} \sim 4\times10^{-8}\,{\rm cm\,s^{-2}}. \quad (2)$$

Thus, the characteristic acceleration scale inherent in stellar feedback physics, $g_{\rm crit} \sim \langle \dot{p}/m_* \rangle$, is of the order of the observed characteristic acceleration of disc galaxies, $g_\dagger = 1.2\times10^{-8}{\rm cm\,s^{-2}}$.

Consider now what happens in different limits of the gravitational acceleration, as implied by equation (2). If $g_{\rm tot} \ll g_{\rm crit}$, then $M_{*,\,\rm young}/M_{\rm gas,\,expelled} \ll 1$ and the fraction of the total gas mass converted to stars is small. Thus, if DM initially dominates $M_{\rm tot}(<R)$, it will generally continue to do so. In the opposite limit, where $g_{\rm tot} \gg g_{\rm crit}$, the SFE is high and baryons cannot escape the galaxy. In such an instance, where feedback is ineffective, dissipative gas accretion within DM haloes is easily sufficient to allow baryonic matter to dominate over DM (Fall & Efstathiou 1980; Katz, Weinberg & Hernquist 1996). This argument implies that a constant characteristic acceleration $g_{\rm crit} \sim g_\dagger$ *should demarcate the transition between the baryon-dominated and DM-dominated regions of a galaxy.*

In our toy model, we have applied equation (1) to a single starburst event, similar to the 'monolithic collapse' model of galaxy formation (Eggen, Lynden-Bell & Sandage 1962). Strictly speaking, within the modern hierarchical paradigm of galaxy formation, this only describes phases of star formation that are 'bursty' on the scale of the entire galaxy. However, we emphasize that the important factors here are the dimensionality and magnitude of $g_{\rm crit}$. The scaling of the SFE may therefore generalize to the more modern galaxy formation picture in which, for most galaxies, most of the stellar mass forms from gas that is continuously accreted from the intergalactic medium. This is predicted to be the case for practically all galaxies in the mass range observed to conform to the baryonic Tully–Fisher relation (BTFR) and RAR (e.g. Rodriguez-Gomez et al. 2016; Anglés-Alcázar et al. 2017).

2.3 Accelerations in the DM-dominated ('deep-MOND') limit and flat rotation curves

In the previous section, we argued that, at large accelerations $g_{\rm tot} \gg g_\dagger$, the total mass is expected to be dominated by baryons and therefore $g_{\rm tot} = G\,M_{\rm tot}(<R)/R^2 \approx g_{\rm baryon} \equiv GM_{\rm bar}(<R)/R^2$ [where $M_{\rm bar}(<R)$ is the baryonic mass enclosed in R], as is indeed observed. Consider now the low-acceleration ('deep MOND') regime, $g_{\rm tot} \ll g_\dagger$. In this regime, the accelerations are observed to scale approximately as $g_{\rm tot} \approx (g_{\rm baryon}\,g_\dagger)^{1/2}$ (e.g. Lelli et al. 2017). Equivalently (since $g_{\rm tot} = V_{\rm c}^2/R$ in terms of the circular velocity $V_{\rm c}$), $V_{\rm c} \approx (G M_{\rm bar}(<R)\,g_\dagger)^{1/4}$. If we make the assumption that $M_{\rm bar}(<R)$ is approximately the total baryonic mass ($\equiv M_{\rm bar}$), e.g. at sufficiently large radii that the baryonic mass starts to converge, then rotation curves are asymptotically 'flat' ($V_{\rm c} \rightarrow$ constant as $R \rightarrow \infty$), with a universal scale $g_\dagger$ above which $g_{\rm tot} \approx g_{\rm baryon}$.

However, in the limit $g_{\rm tot} \ll g_\dagger$, our equation (2) implies that the stellar mass $M_* \sim (g_{\rm tot}/g_{\rm crit})\,M_{\rm gas,\,initial} \approx (g_{\rm tot}/g_{\rm crit})\,f_{\rm bar}^0 M_{\rm tot}$, where $f_{\rm bar}^0 \equiv M_{\rm gas,\,initial}/M_{\rm tot}$ refers to the initial 'total' supply of baryons.[3]

[2] If instead of the non-equilibrium derivation of equation (1), one considers a time-steady galactic SFR $\dot{M}_*$ and wind mass-loss $\dot{M}_{\rm out}$ with momentum flux $\dot{M}_{\rm out}\,v_{\rm escape} \sim \langle p/m_* \rangle \dot{M}_* \sim \langle \dot{p}/m_* \rangle\,M_{*,\,\rm young}$ (where $\langle p/m_* \rangle = \int \langle \dot{p}/m_* \rangle\,dt \sim t_*\langle \dot{p}/m_* \rangle$ for a single stellar population), one obtains the usual momentum-driven wind scaling $\dot{M}_{\rm out} \propto 1/v_{\rm escape}$ (e.g. Murray et al. 2005; Davé, Oppenheimer & Finlator 2011) and we can write $M_*/M_{\rm gas,\,expelled} \sim \langle \dot{M}_* \rangle/\langle \dot{M}_{\rm out} \rangle \sim v_{\rm escape}/\langle p/m_* \rangle \sim (t_*\,\Omega)^{-1}\,(g_{\rm tot}/g_{\rm crit})$, where $t_*\,\Omega \sim 1$ is a correction applicable when $\Omega^{-1} \gtrsim t_*$.

[3] Since the SFE is low in this regime, the expelled gas mass is close to the total initial gas mass.

Solving for the total mass,

$$M_{\rm tot}(<R) \approx \left(\frac{g_{\rm crit}}{g_{\rm tot}}\right)\frac{M_*}{f_{\rm bar}^0} \approx \left(\frac{g_{\rm crit}}{g_{\rm tot}}\right)\frac{(1-f_{\rm g})}{f_{\rm bar}^0}M_{\rm bar}, \tag{H}$$

where $f_{\rm g} = M_{\rm gas}^{\rm relic}/(M_{\rm gas}^{\rm relic} + M_*)$ is the gas fraction determined by the 'relic' gas mass $M_{\rm gas}^{\rm relic}$ that remains after expulsion by stellar feedback. Using the above relations, standard Newtonian dynamics imply that the total acceleration $g_{\rm tot} = g_{\rm Newtonian}$ is

$$g_{\rm tot} \approx \frac{GM_{\rm tot}(<R)}{r^2} \approx \left(\frac{g_{\rm crit}}{g_{\rm tot}}\right)\frac{(1-f_{\rm g})}{f_{\rm bar}^0}\frac{GM_{\rm bar}}{R^2} = \left(\frac{\tilde{g}_{\rm crit}}{g_{\rm tot}}\right)g_{\rm baryon} \tag{4}$$

$$\Rightarrow g_{\rm tot} \approx \left(g_{\rm baryon}\,\tilde{g}_{\rm crit}\right)^{1/2}, \tag{5}$$

where $\tilde{g}_{\rm crit} \equiv g_{\rm crit}(1-f_{\rm g})/f_{\rm bar}^0$ only differs from $g_{\rm crit}$ at the order unity level.[4] Identifying $\tilde{g}_{\rm crit}$ with $g_\dagger$, this may explain the observed asymptotic scaling for small accelerations.[5]

Thus, not only the characteristic acceleration $g_\dagger$, *but also* the asymptotic scalings at both low and high accelerations that define the observed RAR (and MOND, by construction) can potentially be explained as consequences of how stellar feedback acts. Equivalently, in this picture, the fact that observed rotation curves are approximately flat at large radii does not require a 'conspiracy' or 'coincidence' between baryons and DM: rather, stellar feedback ensures the baryons self-regulate with the scaling needed to ensure approximately flat $V_{\rm c}$.[6]

2.4 Expressing $g_\dagger$ in fundamental constants

According to the picture proposed here, $g_\dagger \sim g_{\rm crit} \sim 0.3\,\langle \dot{p}/m_*\rangle$. However, $\langle \dot{p}/m_*\rangle$ itself can be understood in terms of the stellar initial mass function (IMF) and the physics of massive stars. As discussed in Section 2.1, the stellar population-averaged $\dot{p} \sim L/c$ (i.e. $\langle \dot{p}/m_*\rangle \sim c^{-1}\,(L/M)_{*,\,\rm young}$) for a variety of feedback mechanisms, and the most massive stars dominate the luminosity and feedback. The luminosities of these stars are set by the Eddington limit

$$L_{\rm Edd,\,i} = \frac{4\pi G m_{\rm p} c}{\sigma_{\rm T}} M_{\rm i}, \tag{6}$$

where $M_{\rm i}$ is the mass of an individual massive star and $\sigma_{\rm T}$ is the Thomson cross-section. So, $(L/M)_{*,\,\rm young} \sim f_{\rm massive}\,L_{\rm Edd,\,i}/M_{\rm i}$, where the $f_{\rm massive}$ is the mass fraction in massive stars: to reproduce the more accurate full stellar population calculation for a standard IMF (Leitherer et al. 1999), $f_{\rm massive} \sim 0.03$.[7] Thus, we have $\langle \dot{p}/m_*\rangle \sim f_{\rm massive}\,(4\pi\,G\,m_{\rm p})/\sigma_{\rm T}$. Putting these together, we obtain

$$g_\dagger \sim g_{\rm crit} \sim (4\,f_{\rm massive})\,\frac{Gm_{\rm p}}{\sigma_{\rm T}} \sim 0.1\,\frac{Gm_{\rm p}}{\sigma_{\rm T}} \sim 0.5\,Gm_{\rm p}\left(\frac{m_{\rm e}c}{\alpha h}\right)^2, \tag{7}$$

where the last expression uses $\sigma_{\rm T} \equiv (8\pi/3)(\alpha\hbar c/m_{\rm e}c^2)^2$, in terms of the fine-structure constant α, the Planck constant $\hbar = h/2\pi$, the electron mass $m_{\rm e}$, and the speed of light c.

3 DISCUSSION

3.1 Departures from universality

Recent observational analyses have cast serious doubt upon a *fundamental* RAR to which all galaxies must conform exactly (Rodrigues et al. 2018; Chang & Zhou 2019; Stone & Courteau 2019), contrary to previous claims that the observed scatter is fully consistent with measurement errors (Li et al. 2018). Hence, whatever the origin of $g_\dagger$, it is likely emergent rather than fundamental in nature. This fits with the picture presented in this paper: although $g_{\rm crit}$ sets a characteristic scale, there is no reason why galaxies should conform *exactly* to a single RAR. For example, galaxy formation is the product of both *in situ* star formation and hierarchical merging, with merging becoming increasingly important at higher masses, e.g. for massive elliptical galaxies (e.g. Anglés-Alcázar et al. 2017).

Feedback from active galactic nuclei (AGN), rather than stars, is also expected to be most important in massive galaxies. Interestingly, while lower mass disc galaxies prefer the characteristic acceleration described here, the massive ellipticals do not (though they do preserve 'memory' of the mass profiles of merged galaxies; see Boylan-Kolchin, Ma & Quataert 2005). Thus, effects such as variations in galaxy assembly history and AGN feedback should cause galaxies to deviate from the RAR and BTFR.

3.2 Effect of IMF variations

Another source of scatter would be variations in the IMF: $\dot{p}/m_*$ is sensitive to the massive stellar content of a stellar population, so within a given galaxy the observed $g_\dagger$ could vary with it accordingly.

Random variations in $f_{\rm massive}$ are present in any stellar population 'sampled' from an IMF due to the finite number of stars, but in particular the effect of 'incomplete' sampling of the IMF upon $\dot{p}/m_*$ becomes pronounced for stellar populations less massive than 10^4 M$_\odot$ (Murray & Rahman 2010; Kim, Kim & Ostriker 2016). We thus expect increased scatter in the BTFR and RAR in ultra-faint dwarf galaxies with $M_* < 10^4$ M$_\odot$.

It is also possible for the IMF to vary systematically from one galaxy to another, and for the inferred $g_\dagger$ to vary with it. However, the factor $f_{\rm massive}$ is fairly well constrained in an average sense: if it varied strongly with galaxy or local environmental properties, the slopes and normalizations of the Schmidt–Kennicutt and M_*–$M_{\rm halo}$ relations (which are largely set by feedback in current theories) would be quite different. Furthermore, direct observations are consistent with an IMF that is common to all galaxies (Bastian, Covey & Meyer 2010; Offner et al. 2014). Therefore, while variations in the measured $g_\dagger$ could conceivably be driven by IMF variations, it seems likely that they would be dominated by other sources of variations, such as galactic environment and assembly history.

In so far as the IMF *is* roughly universal across cosmic time and feedback does not depend strongly on factors such as metallicity, the arguments presented above imply that (1) the characteristic acceleration scale should not vary systematically with redshift and (2) the observation that $g_\dagger \approx c\,H_0$ in the low-redshift Universe (Milgrom 1983a) is a numerical coincidence.

[4] At face value, this predicts that the measured $g_\dagger$ in a galaxy should be $\propto(1-f_{\rm g})$. However, this is a toy derivation for a single event star formation event; a real galaxy would form over many such events, making the actual prediction non-trivial.

[5] A similar argument was given in Wheeler et al. (2019), but invoking the observed BTFR instead of the SFE scaling.

[6] We note the factor $(1-f_{\rm g})/f_{\rm bar}^0$ is not exactly constant at large radii (though for a galaxy in an NFW DM halo it varies extremely weakly with radius): this may reflect the fact that observed rotation curves are not perfectly flat (e.g. Salucci & Burkert 2000; Courteau & Dutton 2015).

[7] Krumholz (2011) argues that the form of the IMF, and by extension $f_{\rm massive}$, is also expressible in terms of fundamental constants.

3.3 Additional details from cosmological calculations

In ΛCDM, DM-only simulations predict NFW-like DM profiles with $\rho \propto r^{-1}$ on small scales. In such haloes, the maximum (central) acceleration is nearly constant, $g_{\rm tot}^{\rm cen} \sim 3 \times 10^{-9}$ cm s^{-2} (or central $\Sigma_{\rm DM}^{\rm cen} \sim 100\,{\rm M}_\odot\,{\rm pc}^{-2} < \Sigma_{\rm crit}$), with very weak dependence on halo mass and/or redshift, although the presence of baryons and stellar feedback can strongly alter this (e.g. Navarro, Eke & Frenk 1996; Governato et al. 2010; Oñorbe et al. 2015). A 'pure' dark halo therefore has $g_{\rm tot} \lesssim g_{\rm crit}$ at all radii.[8] However, if all of the available baryons fall in, conservation of specific angular momentum implies circularization in a disc with extent $r \sim \lambda\, R_{\rm vir}$ (where $R_{\rm vir}$ is the virial radius; e.g. Fall & Efstathiou 1980; Mo, Mao & White 1998). The acceleration in the galaxy $g_{\rm tot} \sim 2 \times 10^{-8}\,(1+z)^2$ cm s^{-2} ($\Sigma_{\rm bar} \sim 500\,(1+z)^2\,{\rm M}_\odot\,{\rm pc}^{-2}$) then approaches the critical value. If the baryons lose additional angular momentum, or fall in at high redshift, then the centre can become arbitrarily baryon-dominated in principle.

Properly accounting for the complexities of galaxy formation requires much more detailed modelling. However, of course, this is what cosmological simulations and semi-analytical models do. These calculations have indeed shown that the characteristic acceleration scale $g_\dagger$, and more detailed scaling relations such as the RAR and BTFR, emerge naturally in ΛCDM *provided* the models accurately treat stellar feedback (see references in Section 1). More specifically, previous studies have shown that in ΛCDM models that produce the 'correct' galaxy sizes and masses, the characteristic $g_\dagger$ appears in rotation curves as observed; Wheeler, Hopkins & Doré (2019) showed more explicitly that as long as galaxies are broadly consistent with the observed BTFR, this is essentially guaranteed. And it is well known that stellar feedback with $\langle \dot{p}/m_* \rangle$ similar to the values assumed here, based on standard stellar evolution models, is necessary to reproduce these scaling relations in ΛCDM (e.g. Somerville & Davé 2015). The simple arguments presented in this paper do not supplant these much more detailed and sophisticated calculations. Rather, they help demonstrate that the observed universal acceleration scale of galaxies does not require a 'conspiracy' between many different fine-tuned components nor a modified theory of gravity: *stellar feedback contains a characteristic acceleration* that maps directly to the acceleration scale seen in galaxies.

ACKNOWLEDGEMENTS

We thank James Bullock, Manoj Kaplinghat, and Jonathan Stern for useful discussions, and the anonymous referees for various comments that improved and clarified this work. MYG was supported by the CIERA Postdoctoral Fellowship Program. MBK acknowledges support from NSF grants AST-1517226, AST-1910346, and CAREER award AST-1752913, NASA grant NNX17AG29G, and grants *HST*-AR-13888, *HST*-AR-13896, *HST*-AR-14282, *HST*-AR-14554, *HST*-AR-15006, *HST*-GO-12914, and *HST*-GO-14191 from the Space Telescope Science Institute, which is operated by AURA, Inc., under NASA contract NAS5-26555. CAFG was supported by NSF through grants AST-1517491, AST-1715216, and CAREER award AST-1652522, by NASA through grant 17-ATP17-0067, and by a Cottrell Scholar Award from the Research Corporation for Science Advancement. Support for PFH was provided by an Alfred P. Sloan Research Fellowship, NSF Collaborative Research Grant #1715847 and CAREER grant #1455342, and NASA grants NNX15AT06G, JPL 1589742, and 17-ATP17-0214.

[8] This alone can explain, in part, why systems with $g_{\rm tot} \gg g_\dagger$ must be baryon-dominated, but it does not explain why systems with $g_{\rm tot} \ll g_\dagger$ could not also be baryon-dominated.

REFERENCES

Agertz O., Kravtsov A. V., Leitner S. N., Gnedin N. Y., 2013, ApJ, 770, 25
Anglés-Alcázar D. et al., 2017, MNRAS, 470, 4698
Bastian N., Covey K. R., Meyer M. R., 2010, ARA&A, 48, 339
Bershady M. A., Martinsson T. P. K., Verheijen M. A. W., Westfall K. B., Andersen D. R., Swaters R. A., 2011, ApJ, 739, L47
Bosma A., 1981a, AJ, 86, 1791
Bosma A., 1981b, AJ, 86, 1825
Boylan-Kolchin M., Ma C.-P., Quataert E., 2005, MNRAS, 362, 184
Bruzual G., Charlot S., 2003, MNRAS, 344, 1000
Chang Z., Zhou Y., 2019, MNRAS, 486, 1658
Clark P. C., Glover S. C. O., 2014, MNRAS, 444, 2396
Colin P., Vázquez-Semadeni E., Gómez G. C., 2013, MNRAS, 435, 1701
Colín P., Vázquez-Semadeni E., Gómez G. C., 2013b, MNRAS, 435, 1701
Courteau S., Dutton A. A., 2015, ApJ, 801, L20
Davé R., Oppenheimer B. D., Finlator K., 2011, MNRAS, 415, 11
Dekel A., Silk J., 1986, ApJ, 303, 39
Dutton A. A., Macciò A. V., Obreja A., Buck T., 2019, MNRAS, 485, 1886
Efstathiou G., 2000, MNRAS, 317, 697
Eggen O. J., Lynden-Bell D., Sandage A. R., 1962, ApJ, 136, 748
Fall S. M., Efstathiou G., 1980, MNRAS, 193, 189
Fall S. M., Krumholz M. R., Matzner C. D., 2010, ApJ, 710, L142
Faucher-Giguère C.-A., Quataert E., Hopkins P. F., 2013, MNRAS, 433, 1970
Garaldi E., Romano-Díaz E., Porciani C., Pawlowski M. S., 2018, Phys. Rev. Lett., 120, 261301
Gavagnin E., Bleuler A., Rosdahl J., Teyssier R., 2017, MNRAS, 472, 4155
Geen S., Soler J. D., Hennebelle P., 2017, MNRAS, 471, 4844
Geen S., Watson S. K., Rosdahl J., Bieri R., Klessen R. S., Hennebelle P., 2018, MNRAS, 481, 2548
Governato F. et al., 2010, Nature, 463, 203
Grudić et al., 2019, MNRAS, 488, 1501
Grudić M. Y., Hopkins P. F., 2019, MNRAS, 488, 2970
Grudić M. Y., Hopkins P. F., Faucher-Giguère C.-A., Quataert E., Murray N., Kereš D., 2018, MNRAS, 475, 3511
Hayward C. C., Hopkins P. F., 2017, MNRAS, 465, 1682
Hopkins P. F., Grudić M. Y., 2019, MNRAS, 483, 4187
Hopkins P. F., Quataert E., Murray N., 2011, MNRAS, 417, 950
Hopkins P. F., Quataert E., Murray N., 2012a, MNRAS, 421, 3488
Hopkins P. F., Quataert E., Murray N., 2012b, MNRAS, 421, 3522
Kaplinghat M., Turner M., 2002, ApJ, 569, L19
Katz N., Weinberg D. H., Hernquist L., 1996, ApJS, 105, 19
Keller B. W., Wadsley J. W., 2017, ApJ, 835, L17
Kennicutt R. C., Evans N. J., 2012, ARA&A, 50, 531
Kim C.-G., Ostriker E. C., 2015, ApJ, 802, 99
Kim J.-G., Kim W.-T., Ostriker E. C., 2016, ApJ, 819, 137
Kim J.-G., Kim W.-T., Ostriker E. C., 2018, ApJ, 859, 68
Kruijssen J. M. D. et al., 2019, Nature, 569, 519
Krumholz M. R., 2011, ApJ, 743, 110
Krumholz M. R., McKee C. F., Bland-Hawthorn J., 2019, ARA&A, 57, 227
Larson R. B., 1974, MNRAS, 169, 229
Leitherer C. et al., 1999, ApJS, 123, 3
Lelli F., McGaugh S. S., Schombert J. M., Pawlowski M. S., 2017, ApJ, 836, 152
Li P., Lelli F., McGaugh S., Schombert J., 2018, A&A, 615, A3
Li H., Vogelsberger M., Marinacci F., Gnedin O. Y., 2019, MNRAS, 487, 364
Ludlow A. D. et al., 2017, Phys. Rev. Lett., 118, 161103
Martizzi D., Faucher-Giguère C.-A., Quataert E., 2015, MNRAS, 450, 504
Milgrom M., 1983a, ApJ, 270, 365
Milgrom M., 1983b, ApJ, 270, 371
Milgrom M., 1983c, ApJ, 270, 384

Mo H. J., Mao S., White S. D. M., 1998, MNRAS, 295, 319
Murray N., Rahman M., 2010, ApJ, 709, 424
Murray N., Quataert E., Thompson T. A., 2005, ApJ, 618, 569
Murray N., Quataert E., Thompson T. A., 2010, ApJ, 709, 191
Navarro J. F., Eke V. R., Frenk C. S., 1996, MNRAS, 283, L72
Navarro J. F., Benítez-Llambay A., Fattahi A., Frenk C. S., Ludlow A. D., Oman K. A., Schaller M., Theuns T., 2017, MNRAS, 471, 1841
Offner S. S. R., Clark P. C., Hennebelle P., Bastian N., Bate M. R., Hopkins P. F., Moraux E., Whitworth A. P., 2014, in Beuther H., Klessen R. S., Dullemond C. P., Henning T., eds, Protostars and Planets VI. Univ. Arizona Press, Tucson, p. 53
Oñorbe J. et al., 2015, MNRAS, 454, 2092
Orr M. E. et al., 2018, MNRAS, 478, 3653
Ostriker E. C., Shetty R., 2011, ApJ, 731, 41
Planck Collaboration VI, 2018, preprint (arXiv:1807.06209)
Raskutti S., Ostriker E. C., Skinner M. A., 2016, ApJ, 829, 130
Rees M. J., Ostriker J. P., 1977, MNRAS, 179, 541
Rey-Raposo R., Dobbs C., Duarte-Cabral A., 2014, MNRAS, 446, L46
Rodrigues D. C., Marra V., del Popolo A., Davari Z., 2018, Nat. Astron., 2, 668
Rodriguez-Gomez V. et al., 2016, MNRAS, 458, 2371
Rubin V. C., Ford W. K.,, Jr, Thonnard N., 1978, ApJ, 225, L107
Rubin V. C., Ford W. K.,, Jr, Thonnard N., 1980, ApJ, 238, 471
Salucci P., Burkert A., 2000, ApJ, 537, L9
Santos-Santos I. M., Brook C. B., Stinson G., Di Cintio A., Wadsley J., Domínguez-Tenreiro R., Gottlöber S., Yepes G., 2016, MNRAS, 455, 476
Semenov V. A., Kravtsov A. V., Gnedin N. Y., 2016, ApJ, 826, 200
Silk J., 1997, ApJ, 481, 703
Smith N., 2014, ARA&A, 52, 487
Somerville R. S., Davé R., 2015, ARA&A, 53, 51
Stone C., Courteau S., 2019, ApJ, 882, 6
Thompson T. A., Quataert E., Murray N., 2005, ApJ, 630, 167
van den Bosch F. C., Dalcanton J. J., 2000, ApJ, 534, 146
Wheeler C., Hopkins P. F., Doré O., 2019, ApJ, 882, 46
Wong T. et al., 2019, ApJ, 885, 50

This paper has been typeset from a TEX/LATEX file prepared by the author.